Atmospheric Research 266 (2022) 105951

Contents lists available at ScienceDirect

Atmospheric Research

journal homepage: www.elsevier.com/locate/atmosres

A case study of heavy $PM_{2.5}$ secondary formation by N_2O_5 nocturnal chemistry in Seoul, Korea in January 2018: Model performance and error analysis

Hyun-Young Jo [a], Hyo-Jung Lee [a], Yu-Jin Jo [b], Gookyoung Heo [c,**], Meehye Lee [d], Joo-Ae Kim [d], Moon-Soo Park [e], Taehyoung Lee [f], Sang-Woo Kim [g], Yong-Hee Lee [h], Cheol-Hee Kim [a,b,*]

[a] Institute of Environmental Studies, Pusan National University, Busan 46241, Republic of Korea
[b] Department of Atmospheric Sciences, Pusan National University, Busan 46241, Republic of Korea
[c] National Air Emission Inventory and Research Center, Ministry of Environment, Cheongju 28166, Republic of Korea
[d] Department of Earth and Environmental Sciences, Korean University, Seoul 08826, Republic of Korea
[e] Department of Climate and Environment, Sejong University, Seoul 05006, Republic of Korea
[f] Department of Environmental Science, Hankuk University of Foreign Studies, Yongin 17035, Republic of Korea
[g] School of Earth and Environmental Sciences, Seoul National University, Seoul 08826, Republic of Korea
[h] Climate & Air Quality Research Department, National Institute of Environmental Research (NIER), Incheon 404170, Republic of Korea

ARTICLE INFO

Keywords:
N_2O_5 heterogeneous chemistry
PBL
Nitrate aerosol
$PM_{2.5}$ forecasting
CMAQ model

ABSTRACT

Heterogeneous hydrolysis of dinitrogen pentoxide (N_2O_5) plays an important role in nighttime nitrate (NO_3^-) formation in urban areas, and sometimes influences the occurrence of heavy $PM_{2.5}$ pollution the next day in the Seoul Metropolitan Area (SMA), Korea. Here, we discuss the heavy $PM_{2.5}$ wintertime episode of January 13–15, 2018, which was mainly induced by nighttime N_2O_5 heterogeneous reaction in the SMA. In our case, we confirmed that nighttime N_2O_5 hydrolysis is the most critical factor in the rapid formation of aerosol nitrate at high levels during the night, which prevailed in the morning of the next day. Our Integrated Process Rate (IPR) analysis showed that nighttime nitrate production in the episode was almost solely attributable to N_2O_5 chemistry, with hourly mean production rates of 0.8 ± 0.4 μg/m^3 per hour in SMA, which is comparable to the daytime nitrate photochemical production rates of 0.9 ± 0.5 μg/m^3 per hour. We also carried out a series of assessment of N_2O_5–driven nitrate formation sensitivity, and relevant errors were quantified by applying different N_2O_5 uptake coefficients in the WRF-CMAQ model. The potential errors of nighttime-average nitrate concentrations induced by N_2O_5 uptake process were assessed from a linear perspective for the planetary boundary layer (PBL) variances caused by four different PBL parameterization schemes: YSU, ACM2, MYJ, and QNSE. The potential error ranges by N_2O_5 uptake process were analyzed to be 2.3 to 3.5 μg/m^3 (~10% relative to the nighttime-average), while biases of PBL simulations from 4 parameterization schemes were 2.3 ± 1.0 μg/m^3, showing similar ranges in our episode. Although N_2O_5–driven heavy $PM_{2.5}$ episodes do not occur often in SMA, our findings suggest the importance of N_2O_5 chemistry in vigorous wintertime nitrate formation and operational prediction errors of such $PM_{2.5}$ episodes, under the premise of enhanced PBL simulation capabilities.

1. Introduction

Heavy pollution of $PM_{2.5}$ (Particulate Matter with the aerodynamic diameter of less than 2.5 μm), particularly secondary $PM_{2.5}$ is one of the most urgent societal issues in Northeast Asia, and national measures to improve $PM_{2.5}$ air quality have been implemented in South Korea (Kim et al., 2017a; Kim et al., 2017b). The South Korean government has established a new standard crisis management manual for $PM_{2.5}$,

* Correspondence to: C. –H. Kim, Department of Atmospheric Sciences, Pusan National University, 30 San, Jangjeon-Dong, Geumjeong-Gu, Busan 609-735, Republic of Korea.
** Correspondence to: G. Heo, National Air Emission Inventory and Research Center, Ministry of Environment, 206, Osongsaengmyeong-ro, Osong-eup, Heungdeok-gu, Cheongju-si, Chungcheongbuk-do, Republic of Korea.
E-mail addresses: gookyoung@korea.kr (G. Heo), chkim2@pusan.ac.kr (C.-H. Kim).

https://doi.org/10.1016/j.atmosres.2021.105951
Received 22 August 2021; Received in revised form 5 November 2021; Accepted 27 November 2021
Available online 30 November 2021

comprising four different levels (attention, caution, alert, and serious) of alert standards and an associated response system in the event of heavy $PM_{2.5}$, defined as daily average concentrations consecutively exceeding 50 μg/m^3 on multiple days. Because atmospheric processes relevant to heavy $PM_{2.5}$ are highly complex in urban areas (due to meteorological/chemical uncertainties, urban morphology, etc.), a basic understanding of secondary particle formation has become more important (Lee et al., 2019) and is still a challenge for reliable operational $PM_{2.5}$ air quality forecasting.

As themain components of air quality forecasting system, meteorology and chemistry are two major factors in determining the $PM_{2.5}$ concentrations. These two processes are interrelated and sometimes act in a compensatory direction in the comprehensive regional air quality model structure, and thus, numerical sensitivity simulations for reliable predictions are prerequisite. Numerous numerical sensitivity results documented by the National Institute of Environmental Research (NIER) based on failed $PM_{2.5}$ forecasts have shown that the cause of the forecast uncertainty originating from meteorological variables over the 5 years (2015–2019) could be attributed to the wind speed overpredictions (of more than 50%), as well as other factors, such as planetary boundary layer height, wind direction and temperature (NIER, 2018). In particular, wind speed overprediction has frequently occurred in long-range transport cases, and it also becomes important in in urban-scale air quality predictions for high concentrations in stagnant atmospheric conditions in the Seoul Metropolitan Area (SMA), Korea (Park and Kim, 1999; Kim and Ghim, 2002; Park et al., 2004).

The planetary boundary layer (PBL) refers to the lower atmospheric layer, with a depth that is generally less than 2 km, in which human activities take place. PBL has been reported to play an important role in the vertical distribution of air pollutants (Stull, 1988). Previous studies have shown the differences and inconsistencies originating from the PBL parameterization scheme used in modeling studies (Madala et al., 2015; Kim et al., 2015; Banks and Baldasano, 2016; Mohan and Gupta, 2018; Sarkar et al., 2019; Yang et al., 2021). Moreover, the importance and improvement of PBL simulations by turbulence have been highlighted for air pollution modeling in numerous previous studies (Madala et al., 2015; Kim et al., 2015; Mohan and Gupta, 2018; Yang et al., 2021). For example, Kim et al. (2015) studied the sensitivities of the vertical dispersion of pollutants to different PBL schemes using offline meteorology (WRF) and chemistry-transport (Polair3D/Polyphemus) models, and showed that they influence the PM vertical distributions, not only because they influence vertical mixing (PBL height and eddy diffusion coefficient), but also the horizontal wind fields and humidity. Mohan and Gupta (2018) found that PBL parameterization schemes can also have a significant impact on exploring the physical mechanism of the pollution process and predicting the dynamic variations of pollutants, while PBL-$PM_{2.5}$ coupled studies were also performed to examine PBL sensitivity (Su et al., 2018; Lee et al., 2019a; Lee et al., 2019b; Li et al., 2021).

On the other hand, the analysis of errors originating from chemical mechanisms is also important. For example, secondary nitrate (NO_3^-) is an important chemical component of $PM_{2.5,}$ and is recognized to be one of the most highly uncertain factors in predicting $PM_{2.5}$. In the SMA, Korea, the mean concentrations of nitrate have generally been higher than those of sulfate (SO_4^{2-}) in recent years (NIER, 2017; Jo et al., 2020; Kim et al., 2021), while secondary inorganic aerosol (SIA) species are becoming dominant in $PM_{2.5}$ (Pathak et al., 2009; Khan et al., 2010; Squizzato et al., 2012; Shin et al., 2016; Seo et al., 2017). Recently, $PM_{2.5}$ forecasting has also explored considerable uncertainties in the nighttime heterogeneous dinitrogen pentoxide (N_2O_5) chemistry (Prabhakar et al., 2017).

Nevertheless, the error quantifications of general biases induced by chemical processes (i.e., secondary organic/inorganic formation process) are yet to be assessed and remain highly uncertain in $PM_{2.5}$ forecasting. In this context, sensitivity analysis of inorganic species, together with observational studies to validate the simulation, are needed to improve the nitrate formation mechanism over Northeast Asia for the improvement of $PM_{2.5}$ predictions. This is because nitrate is a major component in urban areas, and inaccurate representation of nitrate $PM_{2.5}$ formation chemistry directly results in severely failed $PM_{2.5}$ forecasts.

Nitrate aerosols are formed mainly by two atmospheric pathways: (1) the reaction of OH with NO_2 in the daytime and (2) the N_2O_5 heterogeneous hydrolysis during nighttime (Finlayson-Pitts and Pitts Jr., 1997; Ravishankara, 1997; Finlayson-Pitts and Pitts Jr., 2000; Brown et al., 2006a; Brown et al., 2006b). The product of these two (1) and (2) reactions, HNO_3, is a limiting reagent and/or will thermodynamically partition to the aerosol phase, depending on the ammonia or other inorganic gaseous species (Franchin et al., 2018; Ibikunle et al., 2020; Nenes et al., 2020).

Many previous studies have pointed out that nitrate formation via N_2O_5 heterogeneous hydrolysis is important in producing high $PM_{2.5}$ concentrations, especially during winter, because of the longer nighttime length; thus, the N_2O_5 uptake coefficient (γN_2O_5) is an uncertain, but important parameter in N_2O_5 heterogeneous hydrolysis (Brown et al., 2006a; Baasandorj et al., 2017; Wang et al., 2018). Nevertheless, the extremely high $PM_{2.5}$ (i.e., up to the alert or serious levels of predictions) induced purely by nighttime N_2O_5 formation in urban areas, did not frequently occur in SMA in Korea. However, the heavy $PM_{2.5}$ wintertime episode of January 13–15, 2018, was found to be mainly induced by nighttime N_2O_5 heterogeneous reaction, inferring from the modeling-based estimation of reaction rates for HNO_3 formation and the relevant measurement (NIER, 2018). This made it possible to assess quantitatively the operational $PM_{2.5}$ predictions system capabilities and uncertainties on nitrate formation originating from the N_2O_5 uptake process in SMA.

In this study, we carried out a series of numerical simulations to (1) confirm the importance of the N_2O_5 heterogeneous hydrolysis process in the SMA during nighttime and (2) compare the uncertainty ranges originating from two factors: the N_2O_5 uptake process as an uncertain factor in the chemistry, and the parameterization of PBL height as an uncertain factor in meteorology. We first investigated $PM_{2.5}$ concentrations and weather conditions and selected stagnant winter days for a case study to minimize the wind speed uncertainty in the SMA. N_2O_5 experiments were conducted under the same framework of Jo et al. (2019), and four PBL schemes (YSU, ACM2, MYJ, and QNSE) were employed to quantify the PBL bias, while numerical tests were carried out to evaluate the ranges in PBL errors in the WRF-CMAQ model.

2. Methods and data

2.1. Modeling system and domain

To conduct sensitivity analyses associated with air quality, we adopted the Weather Research and Forecast model (WRF, https://www.mmm.ucar.edu/weather-research-and-forecasting-model) and the United States Environmental Protection Agency's (US EPA's) Community Multi-scale Air Quality model (CMAQ v5.0.2, https://www.cmascenter.org/cmaq/). The WRF (v3.6.1) was used to provide input meteorological fields for the CMAQ (ver. 5.0.2), using the grid nudging technique as a data assimilation method (Bowden et al., 2012; Jeon et al., 2015a). As initial and boundary conditions for the simulations, the 1° × 1° Final Operational Global Analysis (FNL) data of the National Centers for Environmental Prediction (NCEP) were used, and the SAPRC 99 and AERO5 aerosol modules were selected for the gas phase and aerosol phase chemistry, respectively.

The horizontal domain for the WRF-CMAQ simulations comprises three nested domains with horizontal resolutions of 27, 9, and 3 km over the SMA, as shown in Fig. 1. For the vertical resolution, 15 layers were considered with the terrain following sigma coordinates up to 50 kPa. For anthropogenic emissions, Intercontinental Chemical Transport Experiment-Phase B (INTEX-B) inventory for the year 2006 (Zhang

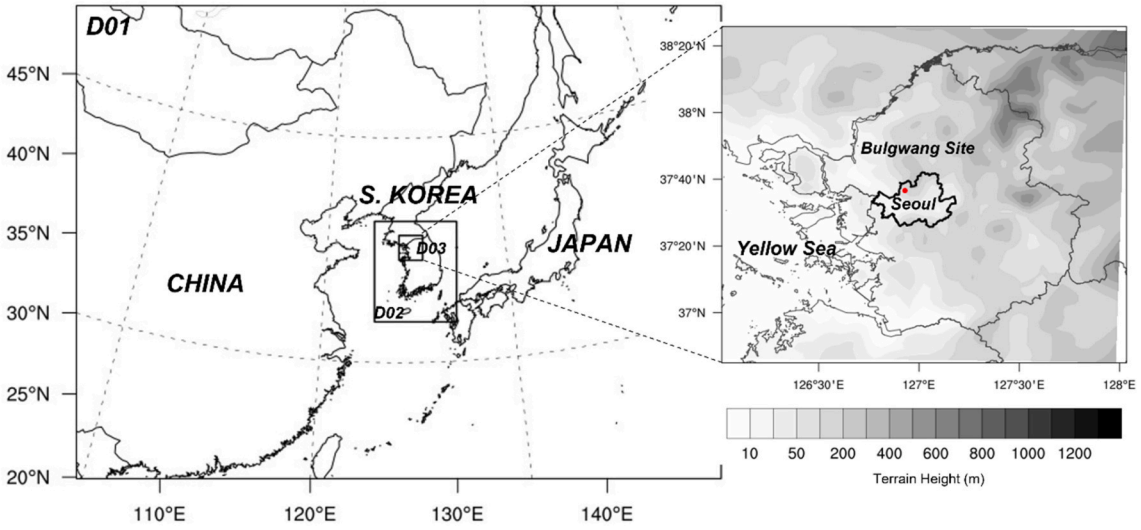

Fig. 1. Modeling domains (27 km, 9 km, and 3 km) and terrain features over the Seoul Metropolitan Area (SMA). The red dot represent Bulgwang supersite in Seoul. (For interpretation of the references to colour in this figure legend, the reader is referred to the web version of this article.)

et al., 2009; Li et al., 2014) was used for Northeast Asia, and Inside South Korea considered here are based on the Clean Air Policy Support System (CAPSS) inventory for the year 2007 (Kim et al., 2008; Lee et al., 2011). The biogenic emissions considered here were based on the Model of Emissions of Gases and Aerosols from Nature (MEGAN) version 2.04 (Guenther, 2006). To evaluate the simulated NO_3^- uncertainties, process analysis with integrated process rates (IPRs) and integrated reaction rates (IRRs) were employed in this study. IPR analysis is a method in WRF-CMAQ model to track contributions of chemical and transport processes to the specific pollutant concentrations, and the IRRs analysis was a technique to investigate chemical sources and losses of pollutants as well as their impact on nitrate formation. Major atmospheric processes such as the emissions of primary species, horizontal transport, vertical transport, gas-phase chemistry, dry deposition, cloud processes, and aerosol processes can all be estimated from IRR analysis.

2.2. Measurements and meteorological data

In-situ measurements and meteorological observations were used to evaluate the performance of the WRF-CMAQ modeling system. Chemical measurements included the total mass and detailed chemical components obtained from the Bulgwang supersite (126.98°E, 37.61°N, 67 m above sea level), as shown in Fig. 1. The Bulgwang supersite is operated by the National Institute of Environmental Research (NIER) and provides various measurements relevant to $PM_{2.5}$ chemical species, such as secondary inorganic aerosol components and trace metal elements data for SMA. Hourly concentrations of $PM_{2.5}$, were measured using the β-ray attenuation method (BAM) (BAM-1020, Met one, USA). As major secondary inorganic aerosol components, water-soluble ions (NO_3^-, SO_4^{2-}, NH_4^+; collectively referred to as SNA) were measured by using an ambient ion monitor (AIM) (URG-9000D, URG Corporation, USA) utilizing ion chromatography. More detailed information can be found in Jeon et al. (2015b).

The meteorological observation data used here include the temperature, relative humidity, wind speed, and wind direction provided by the Korea Meteorological Administration. In addition, we used measured PBL heights, which were estimated using the vertical profiles of the backscattering coefficients from a ceilometer, as well as potential temperatures observed by a microwave radiometer, as described by Park (2018).

2.3. Case selection

Haze events occur frequently during winter in South Korea which were influenced by both local emissions and/or long-range transported air pollutants. Wintertime stagnation conditions could promote secondary aerosol formation and the accumulation of particulate matter, leading to haze events with high concentrations of $PM_{2.5}$. Regarding seasonal features, it is especially important to understand the particulate nitrate formation in winter by N_2O_5 heterogeneous chemistry, due to the longer duration of nighttime than in other seasons. In order to examine the impacts on NO_3^- and $PM_{2.5}$ concentrations by nighttime N_2O_5 heterogeneous chemistry and PBL height, we selected a heavy $PM_{2.5}$ pollution case in winter: January 13–15, 2018, where atmospherically stagnant (with lower wind speed) and relatively high humidity winter days lasted over consecutive days. We excluded 16–18 January 2018 from our case according to the criteria presented by Jo and Kim (2013), where the long-range transport process was dominant.

Fig. 2 shows the hourly variations in $PM_{2.5}$ and Sulfate-Nitrate-Ammonium (i.e., SO_4^{2-}, NO_3^-, and NH_4^+) concentrations measured at the Bulgwang site (Fig. 1) located in the central SMA for the period of January 13–19, 2018. The $PM_{2.5}$ concentrations rapidly increased from January 13 to the afternoon of January 14 (Fig. 2a), mainly because of the accumulation of the local emissions under stagnant atmospheric conditions. However, from the afternoon of January 15, the influence of long-range transport was particularly predominant, and the contribution of domestic sources under stagnant atmospheric conditions was drastically reduced from January 16 to 18.

The speciated chemical compositions of $PM_{2.5}$ measured at the Bulgwang site showed that the SNA component during the case period are 26.6 μg/m^3, accounting for 62.6% of $PM_{2.5}$ mass concentration of 42.3 μg/m^3(Fig. 2b). Among the SNA components, NO_3^- was the major inorganic ion by mass, with an average ratio of NO_3^- to $PM_{2.5}$ of 0.35, which is approximately triple that of SO_4^{2-} (ratio: 0.11) and twice that of NH_4^+ (ratio: 0.16). In Fig. 2c, the neutralization parameter, f_N ($=[NH_4^+]/(2[SO_4^{2-}]+[NO_3^-])$) was employed to diagnose the aerosol acidity. It is recognized that observed f_N was found to be 1.19 (excess aerosol ammonium) in our case. This means no reconciliation with sulfate-nitrate-ammonium aerosol thermodynamics, except for the case of the neutralization of organic acids with ammonia (Dinar et al., 2008; Mensah et al., 2011; Shah et al., 2018), and thus the gas-aerosol partitioning of ammonium nitrate has been established under the 'ammonia-rich' condition. Overall, WRF-CMAQ model simulations also indicated similar f_N (=1.04) to observations, showing the slightly underestimated

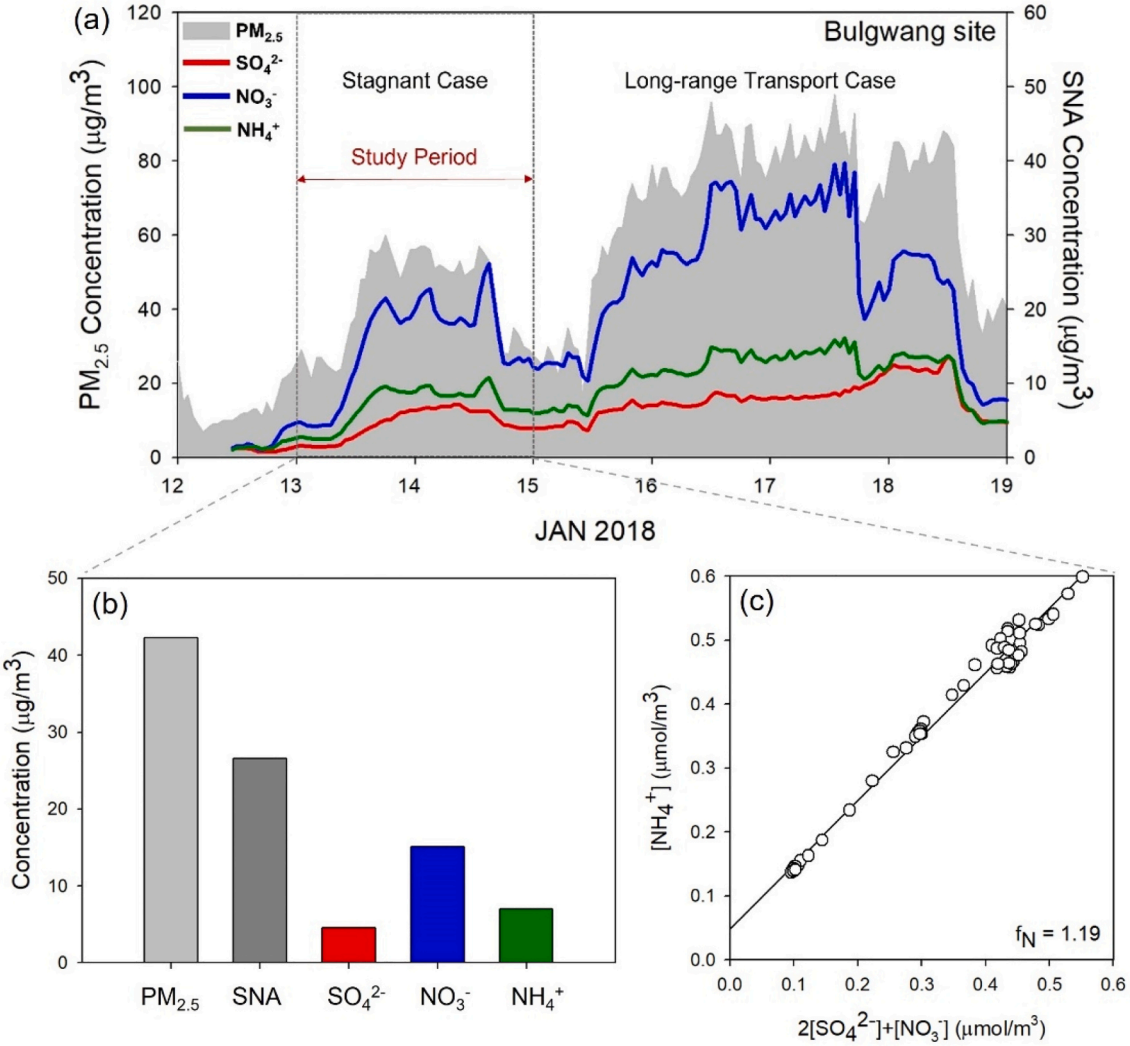

Fig. 2. (a)Temporal variations of measurements, (b) speciated mean mass concentrations of $PM_{2.5}$, SNA, SO_4^{2-}, NO_3^-, and NH_4^+ concentrations measured at Bulkwang site from 12 to 19 January 2018, and (c) acid aerosol neutralization parameter as given by the molar ratio of $[NH_4^+]$ to $2[SO_4^{2-}] + [NO_3^-]$.

neutralization simulated by model for the case.

The hourly variations in $PM_{2.5}$ and NO_3^- concentrations showed similar patterns, and both the $PM_{2.5}$ and NO_3^- concentrations were relatively higher during nighttime than during daytime, which suggests that either nighttime NO_3^- formation or the weak vertical mixing process was an important contributor to the high $PM_{2.5}$ during our selected study period: 1/13/2018 00 LST (15 UTC) to 1/15/2018 00 LST (15 UTC).

2.4. Schemes of PBL sensitivity experiments

To examine the impact of different PBL schemes on $PM_{2.5}$ simulations, four commonly used parameterization schemes; Yonsei University (YSU), Mellor–Yamada–Janjíc (MYJ), quasi-normal scale elimination (QNSE), and the Asymmetric Convective Model, version 2 (ACM2), were implemented in the WRF model in this study. Here, we used YSU as a base case scheme. MYJ and QNSE are classified as turbulent kinetic energy closure schemes that use local vertical gradients to predict turbulent kinetic energy to obtain vertical diffusion coefficients (K_z) as a function of height. The YSU and ACM2 schemes are nonlocal PBL parameterization approaches that estimate PBL height and impose a K_z-profile shape function. Although the comparison results depend on the atmospheric conditions, local approaches tend to perform effectively in stable (or neutral) atmospheric stability conditions, whereas nonlocal approaches simulate an unstable atmosphere more efficiently. Detailed descriptions of these processes have been reported in previous studies (i.e., Hu et al., 2010; Shin and Hong, 2011) and these differences can considerably affect the air quality simulations.

2.5. N_2O_5 heterogeneous chemistry simulation

The N_2O_5 heterogeneous hydrolysis is a major loss pathway for NOx (= NO + NO_2) at night, reducing the amount of NOx available for daytime photochemistry on the following day, while producing nitrate aerosol contributing to $PM_{2.5}$. Reactions (R1) to (R5) show nitrate formation via N_2O_5 heterogeneous hydrolysis. The critical parameters required to determine the impacts of the N_2O_5 uptake processes are the rate constant of reaction (R4), especially the N_2O_5 uptake coefficient (γN_2O_5), which describes the possibility by which the collision of an N_2O_5 molecule with a particle would result in the production of the products of the chemical reaction.

$$NO_{2(g)} + O_{3(g)} \rightarrow NO_{3(g)} + O_{2\ (g)} \quad \text{(R1)}$$

$$NO_{3(g)} + NO_{2(g)} \rightarrow N_2O_{5(g)} \quad \text{(R2)}$$

$$N_2O_{5(g)} \rightarrow NO_{3(g)} + NO_{2(g)} \quad \text{(R3)}$$

$$N_2O_{5(g)} + H_2O_{(het)} \rightarrow 2HNO_{3(aq)} \quad (R4)$$

$$N_2O_{5(g)} + Cl^-_{(het)} \rightarrow Y{\cdot}ClNO_{2(g)} + (2-Y){\cdot}HNO_{3(aq)} \quad (R5)$$

$$HNO_{3(g)} + NH_{3(g)} \rightarrow NH_4NO_{3(s)} \quad (R6)$$

To investigate the impact of the N_2O_5 uptake processes on NO_3^- formation, we performed multiple CMAQ simulations using the framework of Jo et al. (2019). The base case (N_2O_5_ON with YSU PBL scheme) and two sensitivity tests with differing values of γN_2O_5 (C_N_2O_5_ON, changing N_2O_5 heterogeneous chemistry by setting from $\gamma N_2O_5 \times 0.5$ to $\gamma N_2O_5 \times 0.1$) were simulated here. The base case in CMAQ (v.5.0.2) uses a γN_2O_5 parameterization as a function of inorganic particle composition, temperature, and relative humidity (Davis et al., 2008; McDuffie et al., 2018a, 2018b), and the differences between base case minus C_N_2O_5 case ($\triangle C$ = C_N_2O_5 – N_2O_5_ON) represent the impacts of the N_2O_5 heterogeneous uptake process.

3. Results and discussion

3.1. Base case simulation

The simulated meteorological and chemical variables were compared with the measurements at the Bulgwang site, as shown in Fig. 3. For the meteorological variables, 2 m temperature, RH, 10 m wind speed, and PBL height were extracted at the nearest grid point to the Bulgwang site. In Fig. 3, the overall simulated meteorological variables generally showed similar temporal variations with the measurements, with the exception of the underestimated PBL height. The resulting index of agreement (IOA) of 2 m temperature, RH, 10 m wind speed, and PBL height were 0.94, 0.83, 0.57, and 0.50, respectively, indicating that near-surface variables, such as temperature and RH showed more reasonable simulations than wind speed and PBL height.

During the study period, the overall meteorological features showed high RH, low temperature, slow surface wind speed, and low PBL height, which favored the slower dispersion of pollutants, leading to high concentrations of $PM_{2.5}$. However, it should be noted that the mean PBL heights during both daytime and nighttime were underestimated by 66% and 70%, respectively, in our model simulations. Therefore, it could be expected that this underestimation of PBL height would affect the overestimation of $PM_{2.5}$.

The simulation results showed that the concentrations of $PM_{2.5}$, NO_3^-, and NH_4^+, but not SO_4^{2-}, are overestimated for the period of 1/13/2018 00 LST to 1/15/2018 00 LST (Fig. 3). In the current study on the N_2O_5-driven nitrogen chemistry, we did not include the detailed discussion on uncertainties of emission inventories or sulfur chemistry in SMA; these are found in previous studies (Lee et al., 2019a; Kim et al., 2021). The overestimation of $PM_{2.5}$ concentrations was attributed to the overestimation of the daily mean NO_3^- and NH_4^+ by approximately 64% and 30%, respectively. Overestimations were particularly severe for the period of 1/13/2018 18 LST to 1/14/2018 09 LST. In comparison to the underestimation reported by Jo et al. (2019), which used a case in March 2016, this overestimation was partly due to the seasonal feature: winter aerosols tend to have higher concentrations of nitrate and low concentrations of organics, due to both shifts in the thermodynamic equilibrium of ammonium nitrate and reduced oxidation of volatile organic compounds (Wagner et al., 2013). In our case, however, despite existing several other uncertainty factors including SMA's emission strengths of VOC and NO_x, a more important reason for overestimated nitrate (and thus $PM_{2.5}$) is the weak vertical mixing process, mainly due to the underestimated PBL height.

3.2. HNO_3 and NO_3^- concentrations

IPR analysis were conducted at the Bulgwang site to analyze NO_3^-

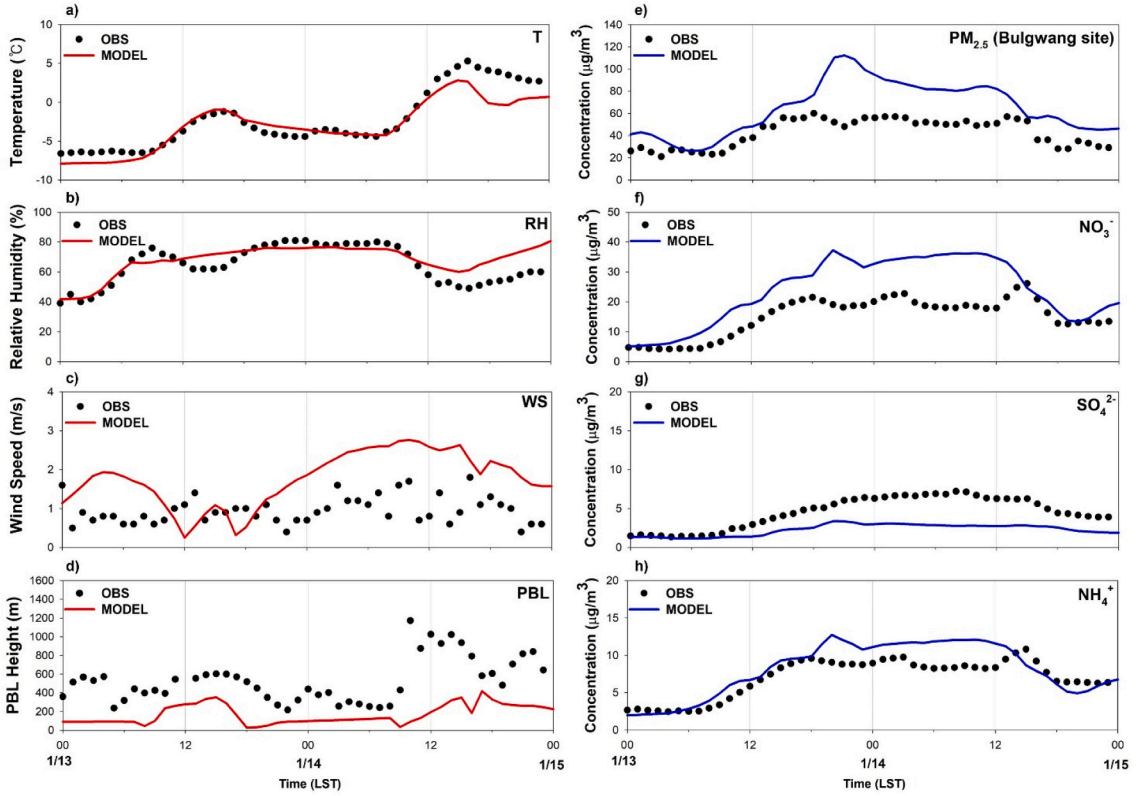

Fig. 3. Comparisons of time series of measurements (black dots) and base case simulations (red line) of temperauture, relative humidity, wind speed, and planetary boundary heigh (PBLH) (left) and $PM_{2.5}$, NO_3^-, SO_4^{2-}, and NH_4^+ concentrations (right) during13–14 January 2018. (For interpretation of the references to colour in this figure legend, the reader is referred to the web version of this article.)

formation to determine which atmospheric chemical/physical processes was more influential. Fig. 4 shows the results of the IPR analysis for HNO_3 (a precursor of NO_3^-), and NO_3^-. In Fig. 4, it is clear that N_2O_5 heterogeneous chemistry accounts for almost all nitrate production

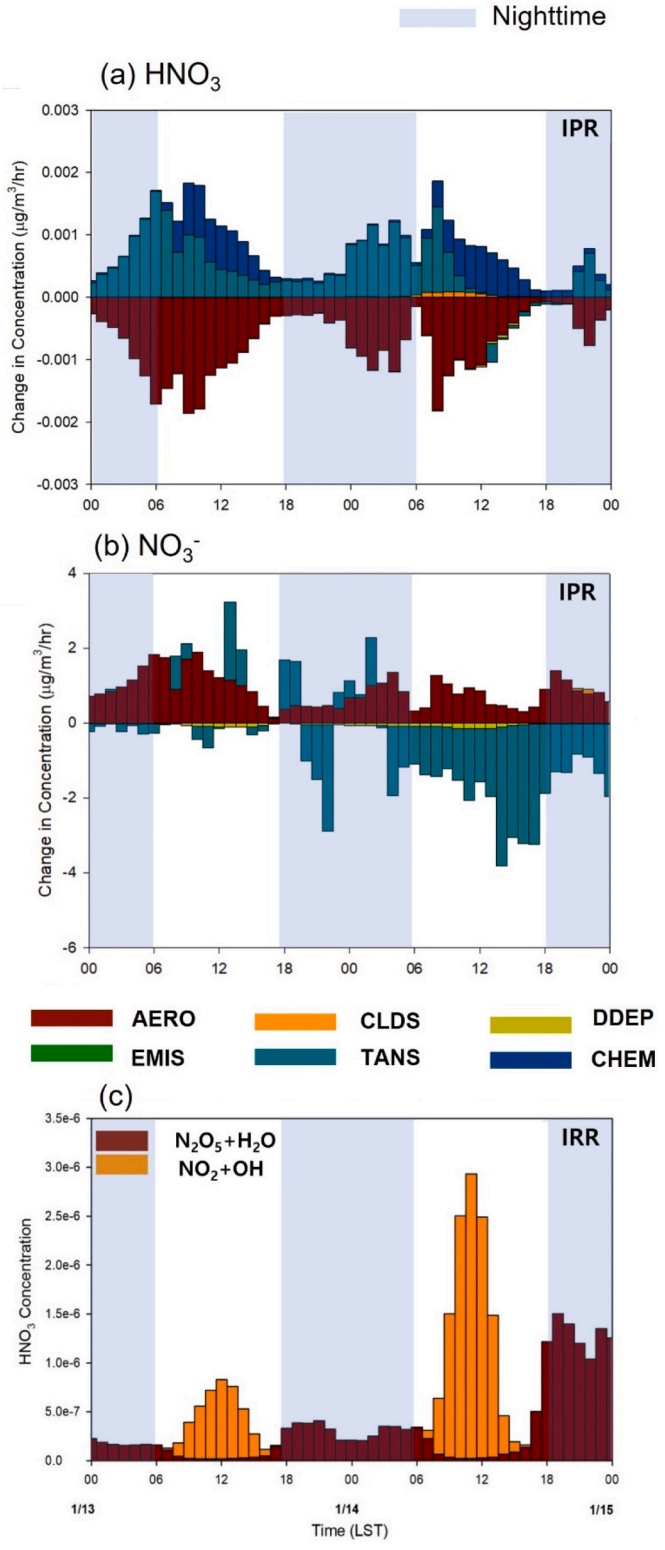

Fig. 4. Time series of integrated process rates for HNO_3 (a) and NO_3^- (b) by aerosol (aero), cloud (clds), dry deposition (ddep), emission (emis) and transport, and integrated reaction rates for HNO_3 formation (c) during 13–14 January 2018.

during the nighttime. Although both the aerosol process (abbreviated as AERO in Fig. 4) and transport process (abbreviated as TRAN in Fig. 4) are the two dominant contributors, they showed the opposite patterns. The opposite contribution of AERO is due to the gas-aerosol equilibrium of NH_4NO_3, where particulate NH_4NO_3 is produced while gaseous HNO_3 is consumed under atmospheric conditions of low temperature and high humidity during nighttime in winter. In our study period, AERO (with the maximum of 1.89 μg/m^3 per hour) contributed to formation of NO_3^- while TRAN (with the maximum of 2.08 μg/m^3 per hour) contributed to loss of HNO_3, indicating that AERO and TRAN processes of NO_3^- are the main two balancing components. During the nighttime, the nitrate production rate was 0.8 ± 0.4 μg/m^3 per hour, which is comparable to a daytime nitrate production rate of 0.9 ± 0.5 μg/m^3 per hour in SMA, again indicating the dominance of nitrate production by the N_2O_5 route, with negligible influences from other processes.

Unlike NO_3^-, the chemical process (abbreviated as CHEM in Fig. 4) showed a positive contribution to HNO_3 during the daytime. This can be interpreted as indicating that HNO_3 was produced by $NO_2 + OH$ through the photochemical oxidation of NOx during the day, and by the $N_2O_5 + H_2O$ process at night, as estimated by the IRR analysis of the gas-phase chemistry module (Fig. 4).

The homogeneous formation of HNO_3 from $N_2O_5(g) + H_2O(g)$ in Fig. 4 is a part of the nitrate formation reaction at night, but proceeds more slowly than the heterogeneous formation of HNO_3 by the heterogeneous hydrolysis of N_2O_5 on and/or within aqueous aerosol particles (Wahner et al., 1998; Ren et al., 2006; Kim et al., 2014; Phillips et al., 2016). It should be noted that the heterogeneous formation of HNO_3 on aerosol was not calculated in the gas-phase chemistry module, but this reaction, together with the reaction relevant to nighttime N_2O_5 heterogeneous chemistry, were all accounted for in the AERO process in the IPR analysis for HNO_3 and NO_3^- (Fig. 4). As a result, the contribution of AERO was found to be significant and pronounced at night, when the NO_3^- concentration increased (or HNO_3 concentration decreased) rapidly (Fig. 4).

3.3. *Vertical distributions of chemical species relevant to N_2O_5 chemistry*

Fig. 5 shows the vertical distributions of NO, NO_2, O_3, NO_3, N_2O_5, and NO_3^- concentrations simulated by base run of WRF-CMAQ. Overall, the vertical distributions showed similar results of Jo et al. (2019) which explained the nighttime NO_3^- formation process by N_2O_5 heterogeneous chemistry. Nevertheless, NO_3 and N_2O_5 showed lower concentrations compared to those reported by Jo et al. (2019), which is partly due to the seasonal characteristics mentioned earlier. Wang et al. (2018) pointed out that NO_3, N_2O_5, and O_3 levels are much lower in winter due to the short daytime length and weak solar radiation.

It should be also noted that the production rate of NO_3^- (in Fig. 5 and Fig. 6) is almost zero at night, whereas, in Fig. 4, large chemical production of HNO_3 or NO_3^- at night was found through N_2O_5 uptake process. This is because the rates were integrated across the PBL in Fig. 4, thereby showing larger chemical production of HNO_3 or NO_3^- through N_2O_5 uptake at night. This is also consistent with the previous studies (Womack et al., 2019; McDuffie et al., 2019) the rate of HNO_3 production was maximized at higher altitudes, as it removed at the surface via NO titration effect caused by higher NO emissions.

The concentration of NO_3, which is mainly formed by the reaction of NO_2 and O_3, was relatively lower in this study because of the reduced O_3 level, and the production of NO_3 was suppressed by the titration of O_3 by NO near the surface. However, the concentrations of N_2O_5 were higher during nighttime and at lower altitudes than NO_3. This is mainly because N_2O_5 was formed by reaction (R2), which requires both NO_3 and NO_2, and NO_2 is more abundant at altitudes closer to the ground level. As the equilibrium partitioning between NO_3 and N_2O_5 is determined by the NO_2 level and ambient air temperature, N_2O_5 is favored by both higher NO_2 concentrations and lower temperature in the current study period. In this study, it was also noted that the simulated NO_3^- concentration

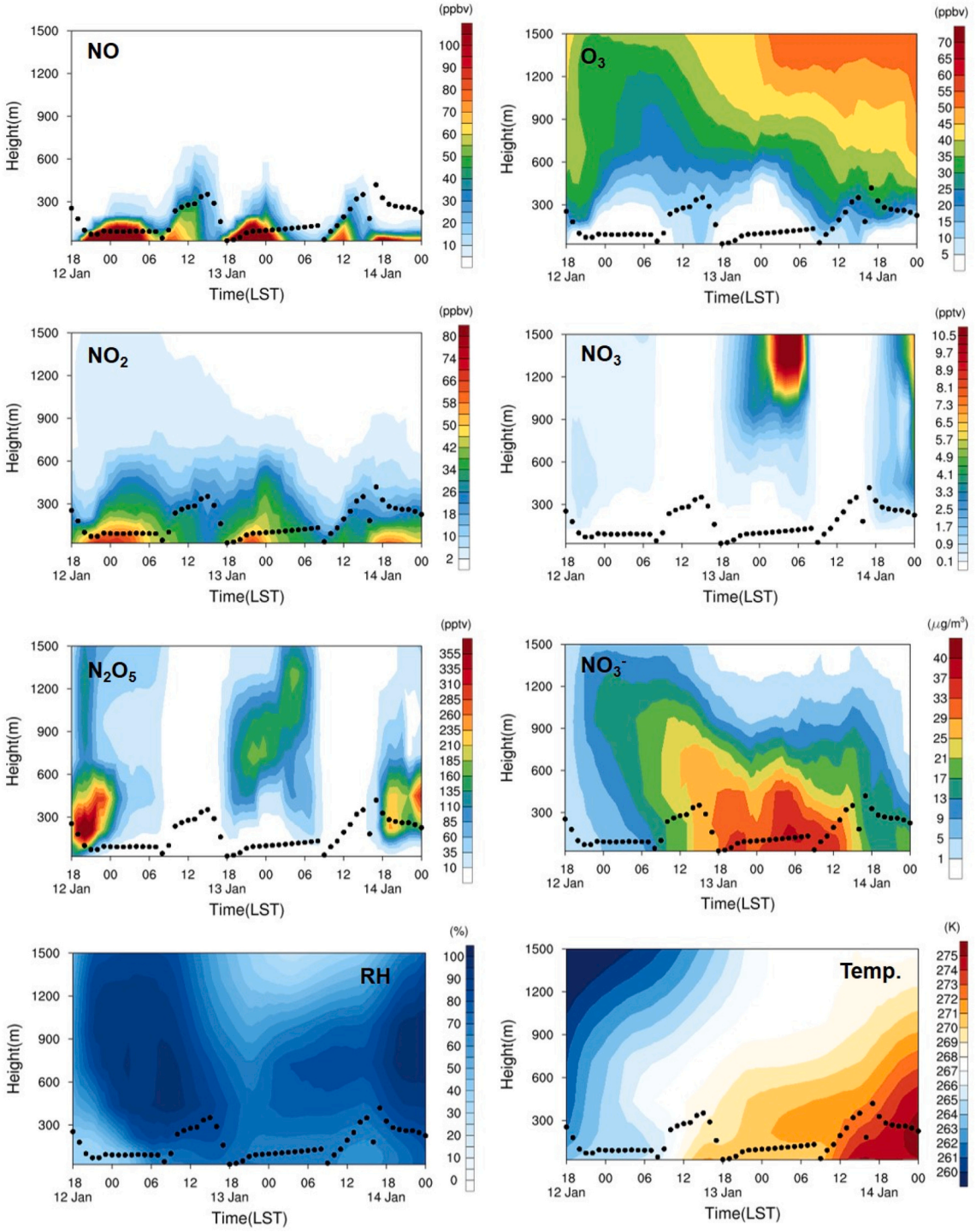

Fig. 5. Time series of vertical NO, O_3, NO_2, NO_3, N_2O_5 and NO_3^- concentrations, relative humidity (RH), and temperature (Temp) during 13–14 January 2018 simulated at Bulkwang site (base case). Black dots (·) represent simulated planetary boundary layer heights.

was higher despite a relatively lower N_2O_5 concentration than that in Jo et al. (2019). This can be attributed to the rapid heterogeneous hydrolysis of N_2O_5, which consumes N_2O_5, produces HNO_3 and subsequently contributes to NO_3^- formation by favorable particle-side partitioning due to low air temperatures in winter.

3.4. Sensitivity analyses of factors influencing simulated $PM_{2.5}$ concentrations

3.4.1. N_2O_5 heterogeneous reaction probability (uptake coefficients)

Fig. 6 shows the time series of $PM_{2.5}$, NO_3^-, and N_2O_5 concentrations from the CMAQ simulations by changing only the N_2O_5 uptake coefficients. The sensitivity results showed lower NO_3^- and $PM_{2.5}$ concentrations in comparison to both the base case (N_2O_5_ON) and C2_N_2O_5_ON cases, as lower N_2O_5 uptake coefficients were used in this study. Compared with N_2O_5_ON simulation, the modeled mean NO_3^-

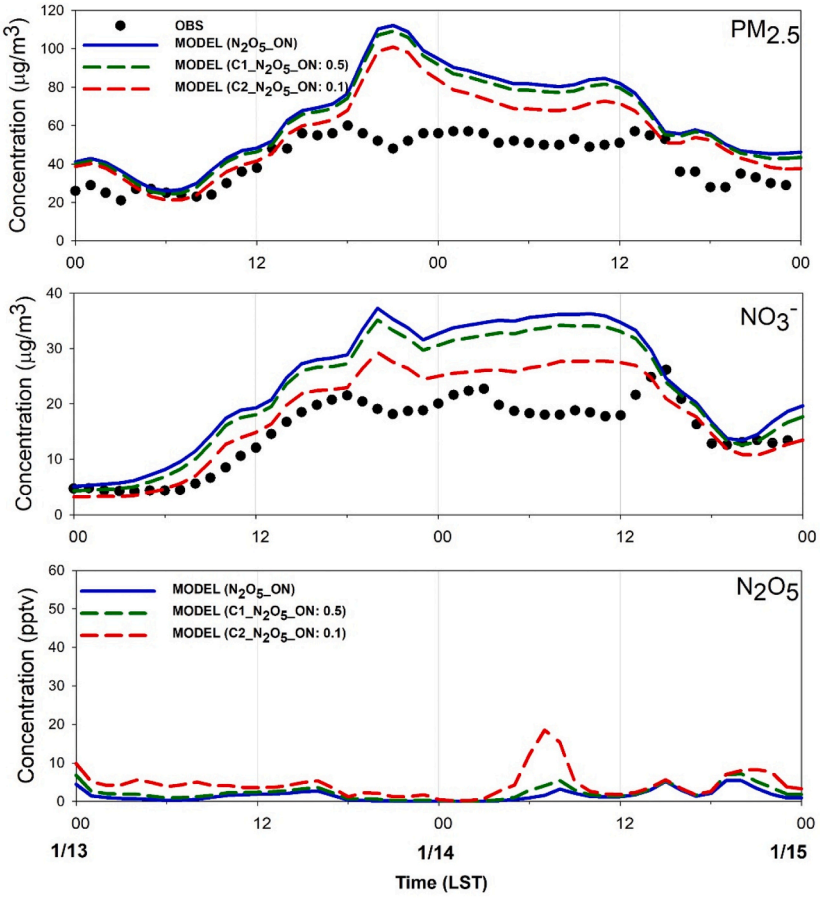

Fig. 6. Time series of measured and modeled $PM_{2.5}$ (a) and NO_3^- (b) concentrations, and modeled N_2O_5 concentrations during 13–14 January 2018 at Bulkwang site (model: N_2O_5_ON (base case), and C_ N_2O_5_ON (base $\gamma N_2O_5 \times 0.5$, base $\gamma N_2O_5 \times 0.1$)).

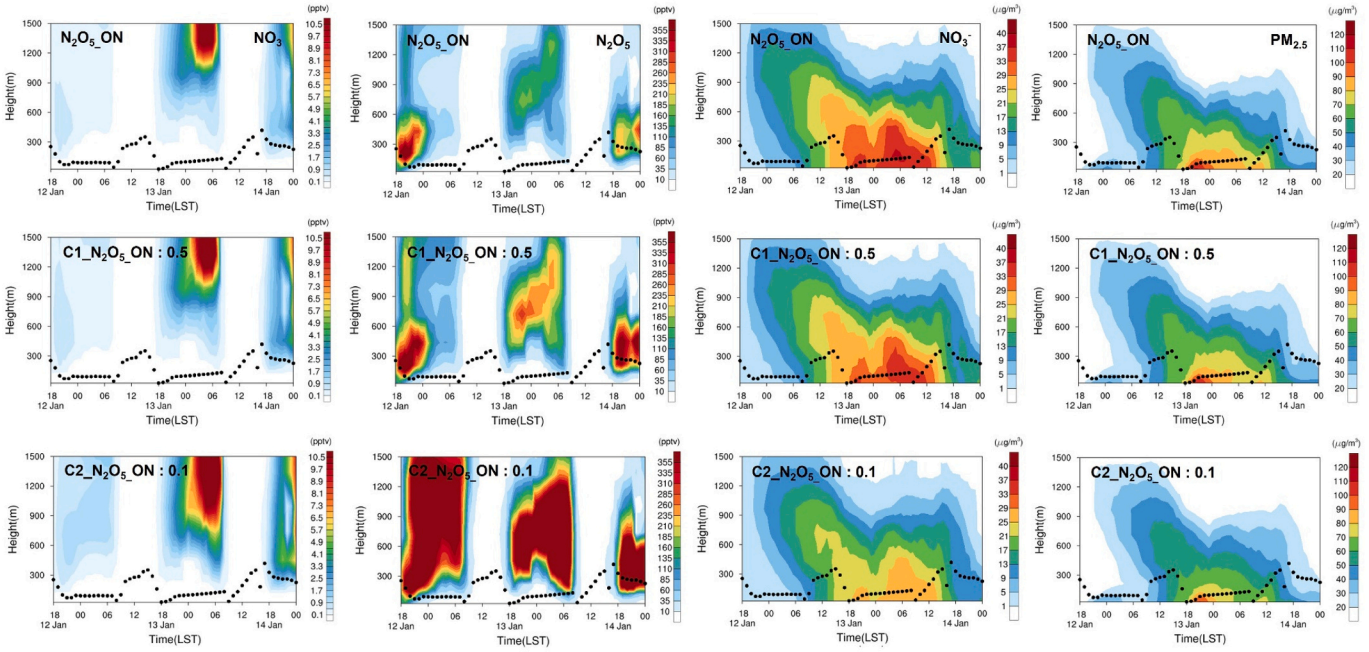

Fig. 7. Time series of vertical NO_3, N_2O_5, NO_3^-, and $PM_{2.5}$ concentrations from 13 to 14 January 2018 at Bulkwang site [model: N_2O_5_ON (base case), and C_ N_2O_5_ON (base $\gamma N_2O_5 \times 0.5$, base $\gamma N_2O_5 \times 0.1$)]. Black dots (·) represent the simulated planetary boundary layer heights.

concentrations in both C1_N_2O_5_ON and C2_N_2O_5_ON simulations decreased by 6.9% (22.2 versus 23.7 μg/m^3) and 30% (18.2 versus 23.7 μg/m^3), respectively; thus, the $PM_{2.5}$ concentrations were also reduced by 3.6% (62.14 versus 64.38 μg/m^3) and 14.24% (56.35 versus 64.38 μg/m^3).

Contrastingly, the N_2O_5 concentration increased due to the reduced N_2O_5 loss, indicating that N_2O_5 can be easily converted to HNO_3 at low temperature and high relative humidity. Considering the relatively large differences in the period from late night on January 13 to early morning on January 14, 2018, it is clear that N_2O_5 heterogeneous chemistry has the potential to build-up NO_3^- with even lower N_2O_5 uptake coefficients.

Fig. 7 shows the vertical variations in the simulated NO_3, N_2O_5, NO_3^-, and $PM_{2.5}$, from N_2O_5_ON (base case), C1_N_2O_5_ON, and C2_N_2O_5_ON at the Bulgwang site. The simulated PBL heights (black dots) are also shown in Fig. 7. The sensitivity simulations showed that NO_3 and N_2O_5 concentrations increased as the N_2O_5 uptake coefficients decreased (C1_N_2O_5_ON and C2_N_2O_5_ON), which was due to the reduction in N_2O_5 removal. The differences in NO_3^- and $PM_{2.5}$ concentrations between N_2O_5_ON and C2_N_2O_5_ON ($\gamma N_2O_5 \times 0.1$) became relatively larger with noticeable differences (18–24 LST on January 13, 2018) as HNO_3 formation via heterogeneous conversion of N_2O_5 decreased.

Our results suggest that the uncertainty in N_2O_5 heterogeneous hydrolysis is the most significant process during the nighttime over the study period. Moreover, our findings indicate that the particulate nitrate formation via N_2O_5 uptake can be the most dominant formation pathway during nighttime in the urban areas of Northeast Asia, such as Seoul, even with a low N_2O_5 uptake coefficient.

3.4.2. PBL

The sensitivity of PBL parameterizations to surface $PM_{2.5}$ concentrations was examined by comparing parameterization schemes. The results showed that biases of wind speed from the four different PBL schemes were more indicative. The MYJ and QNSE-EDMF schemes produced higher wind speed than other schemes (YSU and ACM2), whereas similar performances in the temperature and relative humidity were found between schemes.

Fig. 8 shows the results of the sensitivities from four different PBL schemes, indicating that all schemes, except for QNSE-EDMF, clearly underestimate PBL height over the study period. In particular, the QNSE-EDMF scheme showed relatively better agreement with the measurement, whereas the other three schemes showed a large underestimation of PBL height at night and in the early morning. Table 1 summarizes the evaluated statistical performances by employing the mean Pearson correlation coefficient (R), index of agreement (IOA), root mean square error (RMSE), mean bias (MB), normalized mean bias (NMB), and normalized mean error (NME) for each of the four PBL schemes. The model evaluation parameters found in Emery et al. (2016) and Willmott (1982).

All schemes, except for the QNSE-EDMF scheme, showed overestimated $PM_{2.5}$ and NO_3^- concentrations mainly due to the PBL height underestimation. For example, over the period of 1/13/2018 18 LST to 1/14/2018 09 LST, three other schemes simulated poor diurnal variation of PBL height, while simulated PBL height was immediately reduced as the heat transfer was reduced.

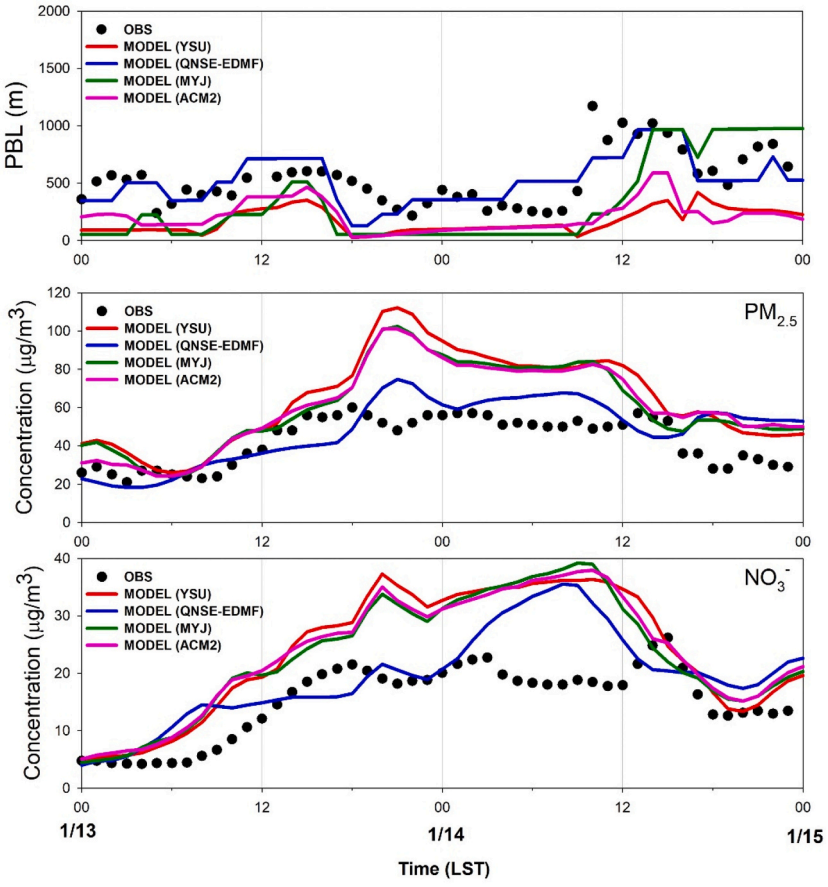

Fig. 8. Time series of measured and modeled planetary boundary height (PBLH), $PM_{2.5}$, and NO_3^- during 13–14 January 2018 at Bulkwang site using the different PBL schemes (YSU, QNSE-EDMF, MYJ, and ACM2).

Table 1
Statistical summary of the simulated and measured planetary boundary layer (PBL) heights.

PBL Schemes		Mean	R	IOA	RMSE	MB	NMB	NME
OBS	All	537.6	.	.	.	.	.	.
	Day	630.6	.	.	.	.	.	.
	Night	450.9	.	.	.	.	.	.
YSU	All	169.9	0.49	0.49	425.4	−356.8	−67.4	67.4
	Day	209.0	0.26	0.49	483.4	−395.3	−64.8	64.8
	Night	126.0	0.76	0.47	355.8	−324.9	−70.9	70.9
MYJ	All	326.9	0.63	0.69	351.0	−199.7	−47.7	62.6
	Day	368.2	0.53	0.66	379.7	−236.1	−45.1	54.6
	Night	258.8	0.84	0.73	303.9	−192.1	−56.5	68.7
ACM2	All	209.8	0.62	0.53	384.1	−316.9	−61.3	61.3
	Day	279.1	0.48	0.54	416.7	−325.3	−54.9	54.9
	Night	142.2	0.72	0.49	342.6	−308.7	−67.3	67.3
QNSE	All	519.1	0.69	0.76	204.5	−7.5	4.94	31.6
	Day	628.7	0.67	0.72	236.8	24.4	7.27	30.1
	Night	409.5	0.55	0.69	165.8	−41.4	2.57	34.0

On daily average, NO_3^- concentration simulated by YSU, MYJ, and ACM2 schemes ranged from 23.2–23.7 μg/m^3, showing overestimation of up to 20% against in-situ measurement of 15.06 μg/m^3. However, unlike the three schemes, the QNSE-EDMF scheme exhibited similar $PM_{2.5}$ and NO_3^- concentrations. The daily average from the QNSE-EDMF scheme is approximately 19.42 μg/m^3, which is reduced by up to 22.5% compared with the other three schemes, YSU, MYJ, and ACM2. Similarly, $PM_{2.5}$ concentrations were decreased by 22%, showing similar levels of measured $PM_{2.5}$ (42.30 μg/m^3). However, the correlation coefficient (R) between the QNSE-EDMF scheme and measurement is relatively lower with a value of 0.68 for NO_3^- and 0.64 for $PM_{2.5}$. This contrasts to the R from other three PBL schemes, such as 0.81–0.87 for NO_3^- (0.80–0.85 for $PM_{2.5}$).

Fig. 9 shows the vertical variations of NO_3, N_2O_5, NO_3^-, and $PM_{2.5}$, at the Bulgwang site from four different PBL schemes against the measured PBL heights. In Fig. 9, relatively noticeable biases were found over the period of 1/13/2018 18 LST to 1/14/2018 06 LST. During the night, three schemes, except for the QNSE-EDMF scheme, underestimated the PBL height with weakened vertical mixing, resulting in higher NO_3^- and $PM_{2.5}$. The QNSE-EDMF showed similar PBL heights and NO_3^- levels to those of the observations due to reasonable vertical dispersion processes.

However, on the morning of the next day, all schemes overestimated $PM_{2.5}$ and NO_3^- concentrations, presumably due to the nighttime NO_3^- formation and the uncertainty of mixing-down process toward the ground level despite the overestimated PBL height. This result implies that PBL height is one of the key factors affecting the improvement of $PM_{2.5}$ predictions. Thus, a very detailed and well-designed

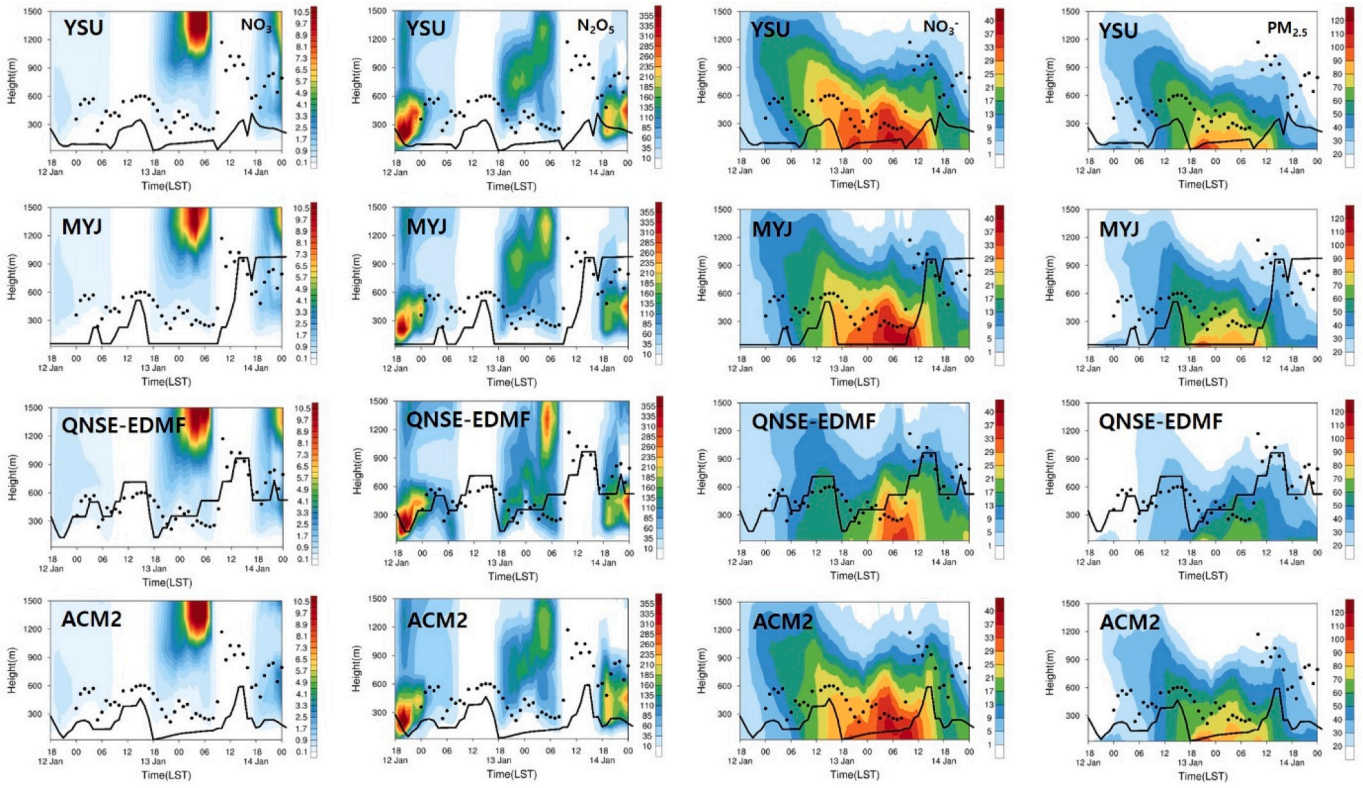

Fig. 9. Time series of modeled vertical NO_3, N_2O_5, NO_3^- and $PM_{2.5}$ concentrations from 13 to 14 January 2018 at Bulkwang site using the different planetary boundary layer (PBL) schemes (YSU, QNSE-EDMF, MYJ, and ACM2). Black dots (·) and black lines represent measured and simulated PBL heights, respectively.

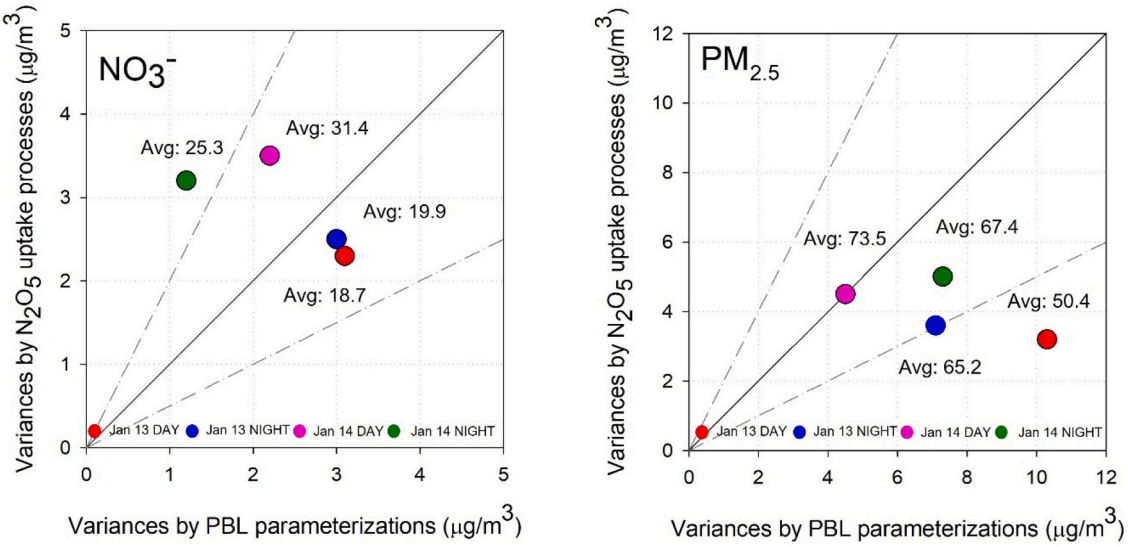

Fig. 10. Ranges in variations originating from the N_2O_5 uptake process vs. planetary boundary layer from four different parameterizations of YSU, QNSE-EDMF, MYJ, and ACM2 schemes during 13–14 January 2018.

measurement-simulation study directly targeting the PBL height and its relevant parameters, such as vertical eddy diffusivity and surface layer flux, would be of great significance for precise nitrate predictions.

Fig. 10 shows the approximate range of errors for the day and night over the study period. We examined the errors originating from both the heterogeneous N_2O_5 uptake process and four different PBL parameterizations for day and nighttime. Here, daytime and nighttime are defined as 07–18 LST and 19–06 LST, respectively. The period-to-period average (from day- and night-time average) changes originating from different N_2O_5 uptake coefficient were found to be 2.3–3.5 μg/m^3 for nitrate (3.2–5.0 μg/m^3 for $PM_{2.5}$), and those from four PBL-schemes were 1.2–3.1 μg/m^3 for nitrate (4.5–10.3 μg/m^3 for $PM_{2.5}$), showing a relatively smaller error range of N_2O_5 uptake process (~10% relative to nighttime average) than the PBL parameterization bias (~15% relative to nighttime average) in our episode.

However, it is difficult to directly compare the bias ranges between the N_2O_5 uptake process and the PBL estimation. This is because the former is the absolute concentration difference between with and without N_2O_5 heterogeneous chemical processes, whereas the latter refers to the relative error estimated from each of the four parameterization schemes. It should also be noted that the magnitude of the bias varies depending on the weather condition variables, such as precipitation, surface wind speed, and other cloud parameters. This may be more exaggerated in higher-emission areas. Nevertheless, the direction and results of our chemistry-meteorology bias-comparison will provide a good basic estimate for the relevant variables for urban areas, or more or less polluted sub-urban areas.

4. Summary and conclusions

This study analyzed the sensitivity of major meteorological and chemical uncertainty factors that greatly affect the accuracy of air quality models. The WRF-CMAQ was applied to simulate experiments on the PBL as a meteorology uncertainty factor and N_2O_5 uptake coefficient as a chemical uncertainty factor to identify the effect on the results of $PM_{2.5}$ numerical simulation in winter. The study period covered January 13–15, 2018, during which the measured NO_3^- concentrations indicated that the nighttime heterogeneous N_2O_5 chemistry accounted for a large fraction of $PM_{2.5}$. We subsequently carried out model sensitivity tests and evaluated the prediction capabilities of $PM_{2.5}$ concentrations by PBL height using four different PBL parameterization schemes and changing γN_2O_5 in the chemistry module of CMAQ.

We first confirmed that nighttime N_2O_5 hydrolysis is the most critical factor at nighttime, and N_2O_5 heterogeneous chemistry has the potential to support the build-up of NO_3^-, even with a lower N_2O_5 uptake coefficient than the default value embedded in the CAMQ model in winter conditions in urban areas, such as Seoul, Korea. The IPR analysis showed that N_2O_5-relevant chemistry accounts for almost all nitrate production during the nighttime with hourly mean production rate of 0.8 ± 0.4 μg/m^3 per hour, comparable to daytime production rate of 0.9 ± 0.5 μg/m^3 per hour, showing ~10% simulations relative to the nighttime average of nitrate.

Other sensitivity experiments with different PBL schemes indicated that the PBL height could be attributed to the performance of simulated $PM_{2.5}$. Unlike the three schemes (YSU, ACM2, and MYJ), the QNSE-EDMF scheme showed PBL heights similar to measurements, and also contributed to improving the performance of simulating NO_3^- and $PM_{2.5}$ concentrations. The QNSE-EDMF scheme showed relatively good model performance at night, which implies the importance of N_2O_5 heterogeneous chemistry and its potential contribution to NO_3^- formation in the urban areas of Northeast Asia, such as Seoul, Korea.

The error ranges of nitrate originating from both the control of the N_2O_5 uptake coefficient and PBL parameterization were found to range from 2.3–3.5 μg/m^3, and 1.2–3.1 μg/m^3, respectively, showing a relatively smaller error range of N_2O_5 uptake process (~10% relative to nighttime average) than the PBL parameterization bias (~15% relative to nighttime average) in the episode studied.

Our results suggest that improving the representation of PBL height and NO_3^- formation by N_2O_5 heterogeneous chemistry contributes to the reasonable simulation of NO_3^- and $PM_{2.5}$ concentrations. However, our case study is a sensitivity test for a limited period; thus, additional modeling and observational studies are needed to precisely predict $PM_{2.5}$ concentrations and forecast $PM_{2.5}$ pollution levels. Given the reasons leading to high $PM_{2.5}$ concentrations that were diagnosed from this study, more general conclusions can be arrived at from much specific PBL characteristics under many environmental conditions, together with the daytime aerosol radiative feedback to the nighttime aerosol (or its precursors) during the aerosol formation processes.

Author statement

H.-Y. Jo, G. Heo, and C.-H. Kim: Conceptualization, M. Lee, J-.A.

Kim, and T. Lee; Data curation M.-S. Park, Y.-H. Lee and S.-W. Kim.; Formal analysis, H.-J. Lee. and Y.-J. Jo.; Investigation, G. Heo.; Methodology, H.-Y. Jo and H.-J. Lee; Visualization, H.-Y. Jo, G. Heo, and C.-H. Kim; Writing—original draft preparation, H.-Y. Jo and C.-H. Kim; Writing—Review and Editing.

Declaration of Competing Interest

The authors declare that they have no known competing financial interests or personal relationships that could have appeared to influence the work reported in this paper.

Acknowledgements

This research was supported by the Basic Science Research Program through the National Research Foundation of Korea (NRF) funded by the Ministry of Education (2020R1A6A1A03044834 and 2020R1I1A1A01072998).

References

Baasandorj, M., Hoch, S.W., Bares, R., Lin, J.C., Brown, S.S., Millet, D.B., Martin, R., Kelly, K., Zarzana, K.J., Whiteman, C.D., Dube, W.P., Tonnesen, G., Jaramillo, I.C., Sohl, J., 2017. Coupling between chemical and meteorological processes under persistent cold-air pool conditions: evolution of wintertime $PM_{2.5}$ pollution events and N_2O_5 observations in Utah's Salt Lake Valley. Environ. Sci. Technol. 51, 5941–5950.

Banks, R.F., Baldasano, J.M., 2016. Impact of WRF model PBL schemes on air quality simulations over Catalonia, Spain. Sci. Total Environ. 572, 98–113.

Bowden, J.H., Otte, T.L., Nolte, C.G., Otte, M.J., 2012. Examining interior grid nudging techniques using two-way nesting in the WRF model for regional climate modeling. J. Clim. 25 (8), 2805–2823.

Brown, S.G., Roberts, P.T., McCarthy, M.C., Lurmann, F.W., 2006a. Wintertime vertical variations in particulate matter (PM) and precursor concentrations in the San Joaquin valley during the California regional coarse PM/Fine PM air quality study. J. Air Waste Manage. Assoc. 56 (9), 1267–1277. https://doi.org/10.1080/10473289.2006.10464583.

Brown, S.S., Ryerson, T.B., Wollny, A.G., Brock, C.A., Peltier, R., Sullivan, A.P., Weber, R. J., Dube, W.P., Trainer, M., Meagher, J.F., Fehsenfeld, F.C., Ravishankara, A.R., 2006b. Variability in nocturnal nitrogen oxide processing and its role in regional air quality. Science 311 (5757), 67–70. https://doi.org/10.1126/science.1120120.

Davis, J.M, Bhave, P.M., Foley, K.M, 2008. Parameterization of N_2O_5 reaction probabilities on the surface of particles containing ammonium, sulfate and nitrate. Atmos. Chem. Phys. 8, 5295–5311.

Dinar, E., Anttila, T., Rudich, Y., 2008. CCN activity and hygroscopic growth of organic aerosols following reactive uptake of ammonia. Environ.Sci.Technol. 42 (3), 793–799.

Emery, C., Liu, Z., Russell, A.G., Odman, M.T., Yarwood, G., Kumar, N., 2016. Recommendations on statistics and benchmarks to assess photochemical model performance. J. Air Waste Manage. Assoc. 67, 582–598.

Finlayson-Pitts, B.J., Pitts Jr., J.N., 1997. Tropospheric air pollution: ozone, airborne toxics, polycyclic aromatic hydrocarbons, and particles. Science. 276 (5315), 1045–1052. https://doi.org/10.1126/science.276.5315.1045.

Finlayson-Pitts, B.J., Pitts Jr., J.N., 2000. Chemistry of the Upper and Lower Atmosphere: Theory, Experiments, and Applications, 969. Academic Press, San Diego. https://doi.org/10.1016/B978-0-12-257060-5.X5000-X.

Franchin, A., Fibiger, D.L., Goldberger, L., McDuffie, E.E., Moravek, A., Womack, C.C., Crosman, E.T., Docherty, K.S., Dube, W.P., Hoch, S.W., Lee, B.H., Long, R., Murphy, J.G., Thornton, J.A., Brown, S.S., Baasandorj, M., Middlebrook, A.M., 2018. Airborne and ground-based observations of ammonium-nitrate-dominated aerosols in a shallow boundary layer during intense winter pollution episodes in northern Utah. Atmos. Chem. Phys. 18 (23), 17259–17276.

Guenther, C.C., 2006. Estimates of global terrestrial isoprene emissions using MEGAN (Model of Emissions of Gases and Aerosols from Nature). Atmos. Chem. Phys. 6, 3181–3210. https://doi.org/10.5194/acp-6-3181-2006.

Hu, X.-M., Nielsen-Gammon, J.W., Zhang, F., 2010. Evaluation of three planetary boundary layer schemes in the WRF model. J. Appl. Meteorol. Climatol. 49, 1831–1844.

Ibikunle, I., Beyersdorf, A., Campuzano-Jost, P., Corr, C., Crounse, J.D., Dibb, J., Diskin, G., Huey, G., Jimenez, J.-L., Kim, M.J., Nault, B.A., Scheuer, E., Teng, A., Wennberg, P.O., Anderson, B., Crawford, J., Weber, R., Nenes, A., 2020. Fine particle pH and sensitivity to NH_3 and HNO_3 over summertime South Korea during KORUS-AQ. Atmos. Chem. Phys. Discuss. https://doi.org/10.5194/acp-2020-501 [preprint]. (in review).

Jeon, W.-B., Choi, Y.-S., Lee, H.-W., Lee, S.-H., Yoo, J.-W., Park, J.-H., Lee, H.-J., 2015a. A quantitative analysis of grid nudging effect on each process of $PM_{2.5}$ production in the Korean Peninsula. Atmos. Environ. 122, 763–774.

Jeon, H., Park, J., Kim, H., Sung, M., Choi, J., Hong, Y., Hong, J., 2015b. The characteristics of $PM_{2.5}$ concentration and chemical composition of Seoul metropolitan and inflow background area in Korea peninsula. J. Korean Soc. Urban Environ. 15, 261–271 (in Korean with English abstract).

Jo, H.-Y., Kim, C.-H., 2013. Identification of long-range transported haze phenomena and their meteorological features over northeast Asia. J. Appl. Meteorol. and Climatol. 52, 1318–1328. https://doi.org/10.1175/JAMC-D-11-0235.1.

Jo, H.-Y., Lee, H.-J., Jo, Y.-J., Lee, J.-J., Ban, J.-L., Chang, L.-S., Heo, G., Kim, C.-H., 2019. Nocturnal fine particulate nitrate formation by N_2O_5 heterogeneous chemistry in Seoul Metropolitan Area, Korea. Atmos. Res. 225, 58–69.

Jo, Y.-J., Lee, H.-J., Jo, H.-Y., Woo, J.-H., Kim, Y., Lee, T., Heo, G., Park, S.-M., Jung, D., Park, J., 2020. Changes in inorganic aerosol compositions over the Yellow Sea area from impact of Chinese emissions mitigation. Atmos. Res. 240, 104948.

Khan, M.F., Shirasuna, Y., Hirano, K., Masunaga, S., 2010. Characterization of $PM_{2.5}$, $PM_{2.5\text{-}10}$ and PM_{10} in ambient air, Yokohama, Japan. Atmos. Res. 96, 159–172. https://doi.org/10.1016/j.atmosres.2009.12.009.

Kim, J.Y., Ghim, Y.S., 2002. Effects of the density of meteorological observations on the diagnostic wind fields and the performance of photochemical modeling in the Greater Seoul area. Atmos. Environ. 36, 201–212.

Kim, S., Moon, N., Byun, D.W., 2008. Korea emissions inventory processing using the US EPA's SMOKE system. Asian J. Atmos. Environ. 2 (1), 34–46, 105572/ajae.2008.2.1.034.

Kim, S., VandenBoer, T.C., Young, C.J., Riedel, T.P., Thornton, J.A., Swarthout, R., Sive, B., Lerner, B.M., Gilman, J.B., Warneke, C., Roberts, J.M., Guenther, A., Wagner, N.L., Dubé, W.P., Williams, E.J., Brown, S.S., 2014. The primary and recycling sources of OH during the NACHTT-2011 campaign. J. Geophys. Res. 119, 6886–6896.

Kim, Y., Sartelet, K., Raut, J.C., Chazette, P., 2015. Influence of an urban canopy model and PBL schemes on vertical mixing for air quality modeling over greater Paris. Atmos. Environ. 107, 289–306.

Kim, H.C., Kim, E., Bae, C., Cho, J.H., Kim, B.-U., Kim, S., 2017a. Regional contributions to particulate matter concentration in the Seoul metropolitan area, South Korea: seasonal variation and sensitivity to meteorology and emission inventory. Atmos. Chem. Phys. 17, 10315–10332. https://doi.org/10.5194/acp-17-10315-2017.

Kim, H.C., Kim, S., Kim, B.U., Jin, C.S., Hong, S.-Y., Park, R.-J., Son, S.-W., Bae, C.-H., Bae, M.-A., Song, C.-K., Stein, Ariel, 2017b. Recent increase of surface particulate matter concentrations in the Seoul Metropolitan Area, Korea. Sci. Rep. 7, 4710. https://doi.org/10.1038/s41598-017-05092-8.

Kim, C.-H., Meng, F., Kajino, M., Lim, J., Tang, W., Lee, J.-J., Kiriyama, Y., Woo, J.-H., Sato, K., Kitada, T., Minoura, H., Kim, J., Lee, K.-B., Roh, S., Jo, H.-Y., Jo, Y.-J., 2021. Comparative numerical study of $PM_{2.5}$ in exit-and-entrance areas associated with transboundary transport over China, Japan, and Korea. Atmosphere 12, 469. https://doi.org/10.3390/atmos12040469.

Lee, D.-G., Lee, Y.-M., Jang, K.-W., Yoo, C., Kang, K.-H., Lee, J.-H., Jung, S.-W., Park, J.-M., Lee, S.-B., Han, J.-S., Hong, J.-H., Lee, S.-J., 2011. Korean national emissions inventory system and 2007 air pollutant emissions. Asian J. Atmos. Environ. 5, 278–291, 105572/ajae.2011.5.4.278.

Lee, D., Choi, J.-Y., Myoung, J., Kim, O., Park, J., Shin, H.-J., Ban, S.-J., Park, H.-J., Nam, K.-P., 2019. Analysis of a severe $PM_{2.5}$ episode in the Seoul metropolitan area in South Korea from 27 February to 7 March 2019: focused on estimation of domestic and foreign contribution. Atmosphere. 10, 756.

Lee, H.-J., Jo, H.-Y., Kim, S.-W., Park, M.-S., Kim, C.-H., 2019a. Impacts of atmospheric vertical structures on transboundary aerosol transport from China to South Korea. Sci. Rep. 9, 1–9.

Lee, H.-J., Jo, H.-Y., Park, S.-Y., Jo, Y.-J., Jeon, W., Ahn, J.-Y., Kim, C.-H., 2019b. A case study of the transport/transformation of air pollutants over the Yellow Sea during the MAPS 2015 campaign. J. Geophys. Res. Atmos. 124, 6532–6553.

Li, M., Zhang, Q., Streets, D.G., He, K.B., Cheng, Y.F., Emmons, L.K., Huo, H., Kang, S.C., Lu, Z., Shao, M., Su, H., Yu, X., Zhang, Y., 2014. Mapping Asian anthropogenic emissions of non-methane volatile organic compounds to multiple chemical mechanism. Atmos. Chem. Phys. 14 (11), 5617–5638. https://doi.org/10.5194/acp-14-5617-2014.

Li, Q.H., Zhang, H.S., Cai, X.H., Song, Y., Zhu, T., 2021. The impacts of the atmosphericboundary layer on regional haze in North China. npj Clim. Atmos. Sci. 4, 9. https://doi.org/10.1038/s41612-021-00165-y.

Madala, S., Satyanarayana, A.N.V., Srinivas, C.V., Kumar, M., 2015. Mesoscale atmospheric flow field simulations for air quality modeling over complex terrain region of Ranchi in eastern India using WRF. Atmos. Environ. 107, 315–328.

McDuffie, E.E., Fibiger Dorothy, L., Dubé William, P., Lopez-Hilfiker, F., Lee Ben, H., Thornton Joel, A., Shah, V., Jaeglé, L., Guo, H., Weber Rodney, J., Michael Reeves, J., Weinheimer Andrew, J., Schroder Jason, C., Campuzano-Jost, P., Jimenez Jose, L., Dibb Jack, E., Veres, P., Ebben, C., Sparks Tamara, L., Wooldridge Paul, J., Cohen Ronald, C., Hornbrook Rebecca, S., Apel Eric, C., Campos, T., Hall Samuel, R., Ullmann, K., Brown Steven, S., 2018a. Heterogeneous N_2O_5 uptake during winter: aircraft measurements during the 2015 WINTER campaign and critical evaluation of current parameterizations. J. Geophys. Res.-Atmos. 123 (8), 4345–4372.

McDuffie, E.E., Fibiger, D.L., Dubé, W.P., Lopez Hilfiker, F., Lee, B.H., Jaeglé, L., Guo, H., Weber, R.J., Reeves, J.M., Weinheimer, A.J., Schroder, J.C., Campuzano-Jost, P., Jimenez, J.L., Dibb, J.E., Veres, P., Ebben, C., Sparks, T.L., Wooldridge, P.J., Cohen, R.C., Campos, T., Hall, S.R., Ullmann, K., Roberts, J.M., Thornton, J.A., Brown, S.S., 2018b. $ClNO_2$ yields from aircraft measurements during the 2015 WINTER campaign and critical evaluation of the current parameterization. J. Geophys. Res.-Atmos. 123 (22), 12,994–13,015.

McDuffie, E.E., Womack, C.C., Fibiger, D.L., Dube, W.P., Franchin, A., Middlebrook, A. M., Goldberger, L., Lee, B.H., Thornton, J.A., Moravek, A., Murphy, J.G., Baasandorj, M., Brown, S.S., 2019. On the contribution of nocturnal heterogeneous reactive nitrogen chemistry to particulate matter formation during wintertime pollution events in Northern Utah. Atmos. Chem. Phys. 19 (14), 9287–9308.

Mensah, A.A., Buchholz, A., Mentel, T.F., Tillmann, R., Kiendler-Scharr, A., 2011. Aerosol mass spectrometric measurements of stable crystal hydrates of oxalates and inferred relative ionization efficiency of water. J. Aerosol Sci. 42, 11–19.

Mohan, M., Gupta, Medhavi, 2018. Sensitivity of PBL parameterizations on PM_{10} and ozone simulation using chemical transport model WRF-Chem over a sub-tropical urban airshed in India. Atmos. Environ. 185, 53–63.

Nenes, A., Pandis, S.N., Weber, R.J., Russell, A., 2020. Aerosol pH and liquid water content determine when particulate matter is sensitive to ammonia and nitrate availability. Atmos. Chem. Phys. 20 (5), 3249–3258.

NIER (National Institute of Environmental Research), 2017. Annual Report of Air Quality in Korea 2016. Seoul, Korea.

NIER (National Institute of Environmental Research), 2018. Annual Report of Air Quality in Korea 2017. Seoul, Korea.

Park, M.S., 2018. Overview of meteorological surface variables and boundary-layer structures in the Seoul metropolitan area during the MAPS-Seoul Campaign. Aerosol Air Qual. Res. 18, 2157–2172. https://doi.org/10.4209/aaqr.2017.10.0428.

Park, S.-U., Kim, C.-H., 1999. A numerical model for the simulation of SO_2 concentrations in the Kyongin region, Korea. Atmos. Environ. 33, 3119–3132.

Park, I.S., Lee, S.J., Kim, C.H., Yoo, C., Lee, Y.H., 2004. Simulating urban-scale air pollutants and their predicting capabilities over the Seoul metropolitan area. J. Air Waste Manage. Assoc. 54 (6), 695–710.

Pathak, R.K., Wu, W.S., Wang, T., 2009. Summertime $PM_{2.5}$ ionic species in four major cities of China: nitrate formation in an ammonia-deficient atmosphere. Atmos. Chem. Phys. 9, 1711–1722. https://doi.org/10.5194/acp-9-1711-2009.

Phillips, G.J., Thieser, J., Tang, M., Sobanski, N., Schuster, G., Fachinger, J., Drewnick, F., Borrmann, S., Bingemer, H., Lelieveld, J., Crowley, J.N., 2016. Estimating N_2O_5 uptake coefficients using ambient measurements of NO_3, N_2O_5, $ClNO_2$ and particle-phase nitrate. Atmos. Chem. Phys. 16 (20), 13231–13249.

Ravishankara, A.R., 1997. Heterogeneous and Multiphase Chemistry in the Troposphere. Science. 276 (5315), 1058–1065. https://doi.org/10.1126/science.276.5315.1058.

Ren, X., Brune, W.H., Mao, J., Mitchell, M.J., Lesher, R.L., Simpas, J.B., Metcalf, A.R., Schwab, J.J., Cai, C., Li, Y., Demerjian, K.L., Felton, H.D., Boynton, G., Adams, A., Perry, J., He, Y., Zhou, X., Hou, J., 2006. Behavior of OH and HO_2 in the winter atmosphere in New York City. Atmos. Environ. 40, 252–263.

Sarkar, A., Sarkar, A., Majumdar, S., 2019. Sensitivity study of planetary boundary layer scheme in numerical simulation of western disturbances over Northern India. SN Appl. Sci. 1, 173.

Seo, J., Kim, J.Y., Youn, D., Lee, J.Y., Kim, H., Lim, Y.B., Kim, Y., Jin, H.C., 2017. On the multiday haze in the Asian continental outflow: the important role of synoptic conditions combined with regional and local sources. Atmos. Chem. Phys. 17, 9311–9332.

Shah, V., Jaeglé, L., Thornton, J.A., Lopez-Hilfiker, F.D., Lee, B.H., Schroder, J.C., Campuzano-Jost, P., Jimenez, J.L., Guo, H., Sullivan, A.P., Weber, R.J., Green, J.R., Fiddler, M.N., Bililign, S., Campos, T.L., Stell, M., Weinheimer, A.J., Montzka, D.D., Brown, S.S., 2018. Chemical feedbacks weaken the wintertime response of particulate sulfate and nitrate to emissions reductions over the eastern United States. Proc. Natl. Acad. Sci. 115 (32), 8110.

Shin, H.H., Hong, S.Y., 2011. Intercomparison of planetary boundary-layer parametrizations in the WRF model for a single day from CASES-99. Bound.-Layer Meteorol. 139, 261–281.

Shin, H.J., Park, S.-M., Park, J.S., Song, I.H., Hong, Y.D., 2016. Chemical characteristics of high PM episodes occuring in spring 2014, Seoul, Korea. Adv. Meteorol. 2016 (1) https://doi.org/10.1155/2016/2424875.

Squizzato, S., Masiol, M., Innocente, E., Pecorari, E., Rampazzo, G., Pavoni, B., 2012. A procedure to assess localand long-range transport contributions to $PM_{2.5}$ and secondary inorganic aerosol. J. Aerosol Sci. 46, 64–76. https://doi.org/10.1016/j.jaerosci.2011.12.001.

Stull, R.B., 1988. An Introduction to Boundary Layer Meteorology. Kluwer Academy, Dordrecht.

Su, T., Li, Z., Kahn, R., 2018. Relationships between the planetary boundary layer height and surface pollutants derived from lidar observations over China: regional pattern and influencing factors. Atmos. Chem. Phys. 18, 15921–15935. https://doi.org/10.5194/acp-18-15921-2018.

Wagner, N.L., Riedel, T.P., Young, C.J., Bahreini, R., Brock, C.A., Dubé, W.P., et al., 2013. N_2O_5 uptake coefficients and nocturnal NO_2 removal rates determined from ambient wintertime measurements. J. Geophys. Res.-Atmos. 118 (16), 9331–9350. https://doi.org/10.1002/jgrd.50653.

Wahner, A., Mentel, T.F., Sohn, M., 1998. Gas-phase reaction of N_2O_5 with water vapor: Importance of heterogeneous hydrolysis of N_2O_5 and surface desorption of HNO_3 in a large teflon chamber. Geophys. Res. Lett. 25 (12), 2169–2172.

Wang, H., Lu, K., Guo, S., Wu, Z., Shang, D., Tan, Z., Wang, Y., Le Breton, M., Lou, S., Tang, M., Wu, Y., Zhu, W., Zheng, J., Zeng, L., Hallquist, M., Hu, M., Zhang, Y., 2018. Efficient N_2O_5 uptake and NO_3 oxidation in the outflow of urban Beijing. Atmos. Chem. Phys. 18, 9705–9721. https://doi.org/10.5194/acp-18-9705-2018.

Willmott, C.J., 1982. Some comments on the evaluation of model performance. B. Am. Meteorol. Soc. 63, 1309–1313.

Womack, C.C., McDuffie, E.E., Edwards, P.M., Bares, R., de Gouw, J.A., Docherty, K.S., Dubé, W.P., Fibiger, D.L., Franchin, A., Gilman, J.B., Goldberger, L., Lee, B.H., Lin, J.C., Long, R., Middlebrook, A.M., Millet, D.B., Moravek, A., Murphy, J.G., Quinn, P.K., Riedel, T.P., Roberts, J.M., Thornton, J.A., Valin, L.C., Veres, P.R., Whitehill, A.R., Wild, R.J., Warneke, C., Yuan, B., Baasandorj, M., Brown, S.S., 2019. An odd oxygen framework for wintertime ammonium nitrate aerosol pollution in urban areas: NOx and VOC control as mitigation strategies. Geophys. Res. Lett. 46 (9), 4971–4979.

Yang, J., Tang, Y., Han, S., Liu, J., Yang, X., Hao, J., 2021. Evaluation and improvement study of the Planetary Boundary-Layer schemes during a high $PM_{2.5}$ episode in a core city of BTH region, China. Sci. Total Environ. 15, 142756, 765.

Zhang, Q., Streets, D.G., Carmichael, G.R., He, K.B., Huo, H., Kannari, A., Klimont, Z., Park, I.S., Reddy, S., Fu, J.S., et al., 2009. Asian emissions in 2006 for the NASA INTEX-B mission. Atmos. Chem. Phys. 9, 5131–5153. https://doi.org/10.5194/acp-9-5131-2009.

Prabhakar, G., Parworth, C.L., Zhang, X., Kim, H., Young, D.E., Beyersdorf, A.J., Ziemba, L.D., Nowak, J.B., Bertram, T.H., Faloona, I.C., Zhang, Q., Cappa, C.D., 2017. Observational assessment of the role of nocturnal residual-layer chemistry in determining daytime surface particulate nitrate concentrations. Atmos. Chem. Phys. 17, 14747–14770. https://doi.org/10.5194/acp-17-14747-2017.co-correspondence (gookyoung@korea.kr) such as; from gookyoung@korea.kr (G.Heo), chkim2@pusan.ac.kr (C.-H. Kim) –> chkim2@pusan.ac.kr (C.-H. Kim), gookyoung@korea.kr (G.Heo)"–>